Tellus (2002), 54A, 34–43
Printed in UK. All rights reserved

TELLUS
ISSN 0280–6495

Effects of hydrostatic approximation and resolution on the simulation of convective adjustment

By DAVID DIETRICH[1] and CHARLES A. LIN[2]*, [1]*Center for Air Sea Technology, Mississippi State University, Stennis Space Center, Mississippi, USA;* [2]*Department of Atmospheric and Oceanic Sciences, and Centre for Climate and Global Change Research (C2GCR), McGill University, and Centre de recherche en calcul appliqué, (CERCA), Montreal, Quebec, Canada*

(Manuscript received 27 December 1999; in final form 20 September 2001)

ABSTRACT

A two-dimensional non-hydrostatic ocean model and a hydrostatic version of the same model are used to simulate convective adjustment, without the use of an instantaneous adjustment parameterization. The model geometry is a domain on the vertical plane of width 40 km and depth 500 m. Model results for four cases are examined: hydrostatic and non-hydrostatic, at 0.1 and 1 km spatial resolution. The convectively adjusted stable state obtained in all four cases are qualitatively similar; thus the hydrostatic approximation does not eliminate convective adjustment. The details of the simulated convective plumes depend on resolution and whether the hydrostatic approximation is made. The adjusted state has significant stratification which cannot be captured by the conventional instantaneous adjustment or diffusion-based parameterizations. We also compare the results to the case when an instantaneous adjustment parameterization is used.

1. Introduction

Convective adjustment in large-scale ocean models is usually parameterized as an instant adjustment process, where static instability is removed instantaneously through vertical mixing or enhanced diffusion. In reality, small-scale non-hydrostatic convective plumes are involved in this adjustment process, and these plumes are not well resolved by coarse resolution hydrostatic models. Lin and Dietrich (1994; hereafter referred to as LD) used a two-dimensional non-hydrostatic model to examine convective plumes. They showed the adjusted state that results from an initial statically unstable state can have significant stable stratification, and is not a well-mixed column as predicted by instantaneous convective adjustment. By the 'adjusted state', we mean the stably stratified state characterised by the occurrence of the first minimum of the potential energy. This minimum occurs as a result of the conversion of potential to kinetic energy of the convective plumes. The non-diffusive behaviour of these plumes cannot be captured using the instantaneous adjustment parameterization. The degree of stratification of the adjusted state depends on the Prandtl number, Pr, the ratio of the eddy viscosity to thermal diffusivity. The instantaneous adjustment used in coarse resolution ocean models corresponds to the limit of $Pr \to 0$, while the case of immiscible fluids corresponds to the limit of large Pr. The latter case has no thermal diffusion, and the adjusted state is stably stratified with the same statistical density distribution as the initial

* Corresponding author.
e-mail: lin@zephyr.meteo.mcgill.ca
Address: Department of Atmospheric and Oceanic Sciences, McGill University, 805 Sherbrooke Street, Montreal, Quebec, Canada H3A 2K6.

state. Convective mixing in the ocean as well as in our numerical model are both characterised by a finite value of *Pr*.

Klinger et al. (1996) examined the evolution of the unstable stratification due to surface cooling in a numerical simulation of oceanic convection, with a cooling timescale of several days. They showed that little stratification develops as the fluid adjusts rapidly to the specified cooling. In this study, we examine convective adjustment from an initial unstable stratified state, with no additional surface cooling. Fernando et al. (1991) performed laboratory experiments to examine the effects of rotation on turbulent convection. Their focus was on the statistical properties of near-equilibrium convecting boundary layers, whereas we address strong transients resulting from strongly unstable initial conditions as may occur in the ocean during an intense surface cooling event. Marshall and Schott (1999) provides a comprehensive review of the theory, modeling and observations of oceanic convection.

The use of non-hydrostatic models to treat the convective scale is discussed by Marshall et al. (1997). They found significant differences between hydrostatic and non-hydrostatic modeling of convective plumes. The lack of vertical inertia in the hydrostatic system gives faster growing plumes and smaller scales for the most unstable modes. All of the potential energy released through convection goes into horizontal kinetic energy, rather than horizontal and vertical kinetic energy. The amount of potential energy available is the same in both hydrostatic and non-hydrostatic formulations, but it is released more quickly under the hydrostatic approximation. The vertical flow in this case is determined by the incompressibility condition, and has no direct energy source. The total kinetic energy in the hydrostatic case remains bounded, as the horizontal velocity is limited by the available potential energy and the vertical velocity is limited through the incompressibility condition. The hydrostatic system is thus numerically stable and can be used to examine convective adjustment.

As Marshall et al. (1997), we use the same basic model for both hydrostatic and non-hydrostatic simulations. This enables us to isolate clearly non-hydrostatic effects. We follow the DieCAST model formulation (Dietrich and Ko, 1994; Dietrich, 1997). Our numerical algorithm used to allow for non-hydrostatic effects is iterative, as is the solution of Marshall et al. of the three-dimensional Poisson equation to satisfy incompressibility. Our iterative procedure, described in the Appendix, is numerically efficient, accurate and stable.

The qualitative details of three-dimensional flows under convective adjustment can be quite different from those in two-dimensions, primarily because of three-dimensional baroclinic instabilities. The roles of instabilities that may occur in three-dimensional convection and how they interact with the large-scale environment are discussed by Haine and Marshall (1998). However, three-dimensional models are unlikely to have sufficient resolution to resolve fully the details of convective adjustment in basin-scale simulations in the near future. This motivates the use of two-dimensional models. Such models can shed light on important questions such as how the hydrostatic approximation and resolution affect the adjusted state, and whether it is possible to extrapolate results from low to high Reynolds numbers. In this study, we focus on the first question, recognizing the limitations of two-dimensional models.

The Coriolis terms were not included in our earlier study LD as they have little effect on the fast timescales of the convective plumes. (However, vortex stretching effects associated with Coriolis effects can severely constrain convection when resolution is inadequate.) We include Coriolis terms in this study, as well as a sloping bottom. This enables us to capture horizontal and vertical temperature gradients and the associated thermal wind in the convectively adjusted state, thereby showing more fully the implications of instant convective adjustment with sloping topography (such as for a coastal polynya). The governing equations are presented in Section 2. They include three velocity components in two dimensions, and are sometimes referred to as being 2.5-dimensional.

We compare the convective adjustment simulated by two-dimensional hydrostatic and non-hydrostatic models, at 0.1 and 1 km resolution. We show the adjusted states in the two models are qualitatively similar, with both being different from that obtained using the instant convective parameterization. The hydrostatic approximation does not eliminate convection in a numerical model. Most ocean models are hydrostatic; thus the effects of the hydrostatic approximation on convective adjustment are of great interest. Note

that by 'convective adjustment', we mean the physical adjustment process itself, without any connotation of instantaneous mixing or enhanced diffusion. The simulations are carried out to longer times than is needed for the bulk of convective adjustment, to show the beginning and ending of the adjustment and the sloshing gravity waves that dominate thereafter. The problem that we examine is similar to that of LD: the adjustment of an unforced two-dimensional fluid with a cold, hence dense, layer on top initially. This corresponds to the limiting case of rapid sudden surface cooling.

2. Model formulation

We use in our study a new, non-hydrostatic version of the z-level, fourth-order accurate modified Arakawa A-grid DieCAST ocean model (Dietrich and Ko, 1994; Dietrich, 1997). The non-hydrostatic model makes use of the Boussinesq approximation. No along-channel flow variation in the x-direction is assumed, thus making the model two-dimensional. The model equations are shown below.

$$u_t = -\nabla \cdot u\boldsymbol{V} + fv + A_{\mathrm{m}} u_{yy} + (\upsilon u_z)_z$$

$$v_t = -\nabla \cdot v\boldsymbol{V} - p_y - fu + A_{\mathrm{m}} v_{yy} + (\upsilon v_z)_z$$

$$\delta w_t = \delta[-\nabla \cdot w\boldsymbol{V} + A_{\mathrm{m}} w_{yy} + (\upsilon w_z)_z] - p_z + g\beta T$$

$$T_t = -\nabla \cdot T\boldsymbol{V} + A_{\mathrm{h}} T_{yy} + (\kappa T_z)_z$$

$$\nabla \cdot \boldsymbol{V} = 0$$

The notation is standard. $\boldsymbol{V} = (v, w)$ is the two-dimensional velocity in the horizontal (y) and vertical (z) directions; subscripts y, z denote partial differentiation; T, p, g, υ, κ, β and f are the temperature, pressure normalized by a reference density, gravitational acceleration, eddy viscosity, thermal diffusivity, thermal expansion coefficient and constant Coriolis parameter, respectively. The symbols ∇ and ∇^2 denote the gradient and Laplacian operators on the vertical plane respectively. δ is a multiplier which takes on the value of 0 or 1 for the hydrostatic and non-hydrostatic case, respectively. The equations are solved using a fourth-order accurate control volume approximation for the horizontal pressure gradient and advection terms. For optimum accuracy, both the Arakawa 'A' and 'C' control volume grids are used, with fourth-order accurate interpolations between them. Further details are given in Dietrich (1997).

The values of the model parameters are as follows. The coefficient of thermal expansion $\beta = 2 \times 10^{-4}\,\mathrm{K}^{-1}$; horizontal viscosity $A_{\mathrm{m}} = 20\,\mathrm{m}^2\,\mathrm{s}^{-1}$; horizontal diffusivity $A_{\mathrm{h}} = 2\,\mathrm{m}^2\,\mathrm{s}^{-1}$, except $A_{\mathrm{h}} = 20\,\mathrm{m}^2\,\mathrm{s}^{-1}$ in the top model layer; background values of vertical viscosity $\upsilon = 10\,\mathrm{cm}^2\,\mathrm{s}^{-1}$ and vertical diffusivity $\kappa = 1\,\mathrm{cm}^2\,\mathrm{s}^{-1}$, except $\kappa = 10\,\mathrm{cm}^2\,\mathrm{s}^{-1}$ at the interface between the top two layers; Coriolis parameter $f = 9.7 \times 10^{-5}\,\mathrm{s}^{-1}$. When finite amplitude convection develops, the vertical viscosity and diffusivity are augmented from their background values, so that the vertical cell Peclet and Reynolds numbers do not exceed 10, as in LD.

The time integration scheme is a modified leap-frog scheme (Dietrich et al., 1987). The solution of the non-hydrostatic model ($\delta = 1$) is obtained iteratively from the hydrostatic solution ($\delta = 0$), as described in more detail in the Appendix.

Our model formulation, based on the DieCAST model, is fourth-order accurate everywhere except in control volumes next to the boundaries, where it is second-order accurate. The fourth-order accuracy greatly reduces numerical overshoots from truncation errors that may occur in regions with a large cell Reynolds or Peclet number. The use of enhanced viscosity and diffusivity values in control volumes adjacent to the top rigid lid boundary emulates the effects of sub-gridscale turbulent mixing near the surface, and reduces numerical overshoots. The generally larger values of the horizontal diffusivity compared to the vertical values represent subgrid scale mixing as the horizontal resolution (100 m) is coarse compared to the vertical resolution (of order 5 m).

Insulated conditions for temperature are used at the boundaries. Free-slip conditions are used at the rigid top and lateral boundaries, with non-linear drag at the bottom. The initial conditions consists of zero flow, with an unstably stratified dense layer extending from the surface to a depth of 100 m, and stable stratification at deeper levels. The temperature difference between the top and bottom of the unstably stratified layer is 4.5 °C. The channel bathymetry is parabolic in the y-direction, with zero depth at the edges, and increasing to a maximum depth of $D = 500$ m at the centre of the channel. Fifty levels are used in

the vertical, with the top layer thickness being 5 m, and increasing smoothly to 17 m at the bottom. The horizontal extent of the domain is $L = 40$ km, with a horizontal resolution of either 0.1 or 1 km.

3. Model results and discussion

We present model results for five cases. The first four consist of the hydrostatic and non-hydrostatic results at a resolution of 0.1 and 1 km without the use of the instantaneous adjustment parameterization, and the fifth uses instantaneous adjustment for the hydrostatic model at 0.1 km resolution. As there is no flow variation in the x-direction, a yz-section on the vertical plane shows the full flow structure.

Figure 1 shows the temperature cross-section during the early development of finite amplitude plumes for the hydrostatic and non-hydrostatic cases with no instantaneous adjustment at 0.1 km resolution. The plumes are resolved by about five horizontal grid points, and are slightly smaller in scale for the hydrostatic case. The lack of vertical inertia in the hydrostatic case favours a larger ratio of vertical to horizontal velocity, and thus smaller horizontal scales. The vertical scale in both cases is the depth of the unstable layer.

Figure 2 shows space–time (y–t) sections of the vertical velocity of layer 12 at a depth of $z =$ 69.7 m for all four cases without instantaneous adjustment. At 0.1 km resolution, we see the earlier appearance of the plumes in the hydrostatic compared to the non-hydrostatic case. The magnitude of the convection is stronger in the hydrostatic case, as measured by the maximum upwelling (39.1 versus 33.5 cm s^{-1}) and downwelling (-27.9 versus -20.8 cm s^{-1}) velocities. Both these effects are due to the absence of vertical inertia in the hydrostatic case. The difference between the hydrostatic and non-hydrostatic results becomes smaller at the coarser resolution of 1 km. This is because non-hydrostatic effects become important only when the horizontal grid size is smaller than the scale of the unstable stratification (Xu and Lin, 1993). The plumes are much weaker in amplitude compared to the high-resolution case, as the fastest growing modes are sub-grid scale and hence not resolved. We note the model is robust in the hydrostatic case without the use of instantaneous convective adjustment to remove static instability.

Figure 3 shows the time evolution of the horizontally (y) averaged temperature. At 0.1 km resolution, the hydrostatic plumes appear earlier, as noted earlier. This results in a quicker establishment of the adjusted state. The adjustment itself is characterised by significant counter-diffusive heat transport. The fluid is materially flipped over by the action of the convective plumes which are finite-amplitude modes of Rayleigh–Taylor instability. For example, the warmest water in Fig. 3a is found at about 100 m depth at just before 2 h. At about 2 h, there is little stratification in the zonally averaged state. After this adjustment stage, the warmest water is found at the surface. Such strongly advective effects cannot be captured by instantaneous adjustment parameterizations. At 1 km resolution, the plumes appear later, and there is little difference between the hydrostatic and non-hydrostatic cases. Note the minimum (5 °C) and maximum (9.4 °C) temperatures reached in the four cases are very similar, as they are determined by the initial conditions. The adjusted state itself is also similar in all four cases, with a stable stratification characterised by non-dimensional temperature contour label varying from 1 to 6.

We now examine the results obtained using an instantaneous adjustment procedure where static instability is removed in one time step, for the hydrostatic case at 0.1 km resolution. This is the traditional parameterization for convective adjustment in large-scale ocean models. The temperature at $t = 1.5$ h, the time evolution of vertical velocity at depth $z = 69.7$ m, and of horizontally averaged temperature are shown in Figs. 4a, b and c, respectively. These should be compared to the corresponding Figs. 1b, 2b and 3b for the hydrostatic case at 0.1 km resolution. The instantaneous adjustment removes the initial static instability immediately, and results in an adjusted state which is qualitatively different from that obtained without using this adjustment.

4. Conclusions

We have shown in this study that it is not necessary to use an instantaneous adjustment procedure, traditionally used in hydrostatic large-

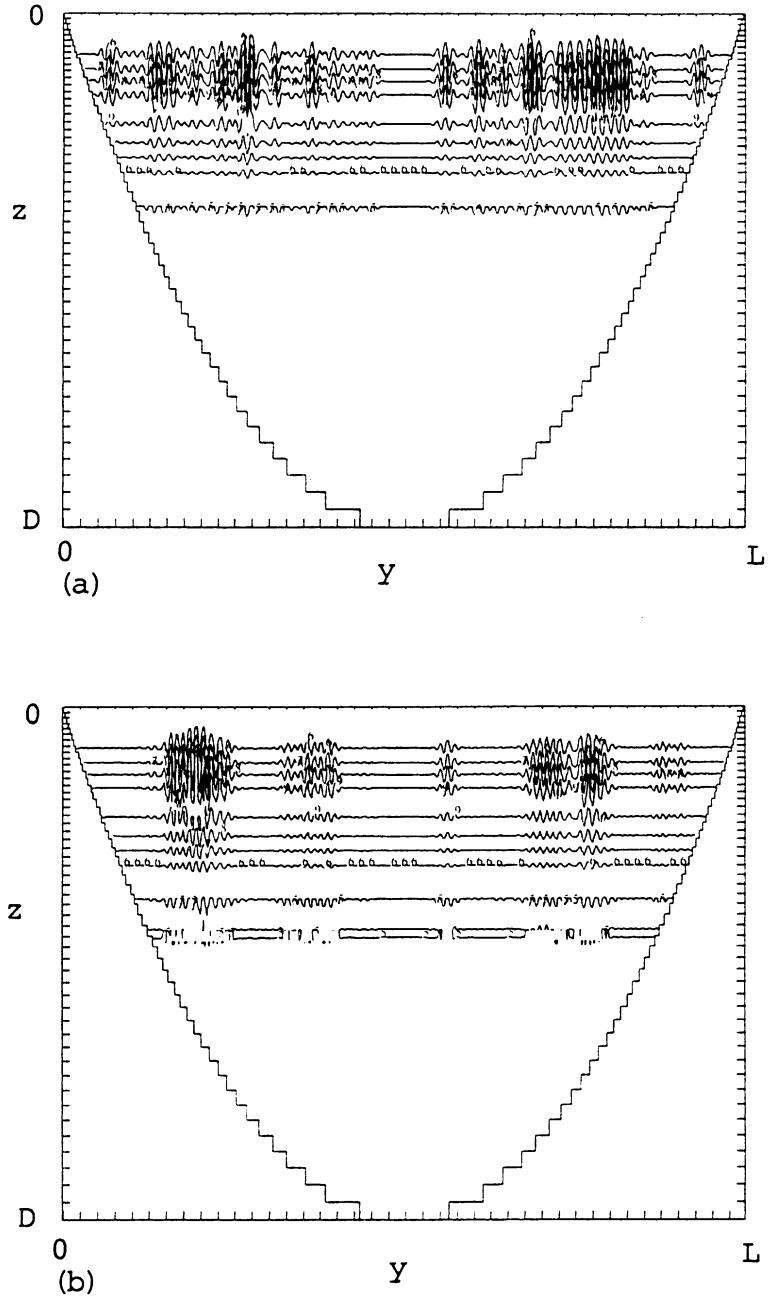

Fig. 1. The temperature cross-section on the vertical (yz) plane at time $t = 1.5$ h for (a) the hydrostatic and (b) the non-hydrostatic case, at a resolution of 0.1 km without instantaneous adjustment. The maximum and minimum temperature (°C) are indicated; the contour labels are in °C. The tick marks on the ordinate show the vertical grid interval increasing smoothly from 5 m at the surface to 17 m at the bottom. The depth $D = 500$ m, and the horizontal extent is $L = 40$ km.

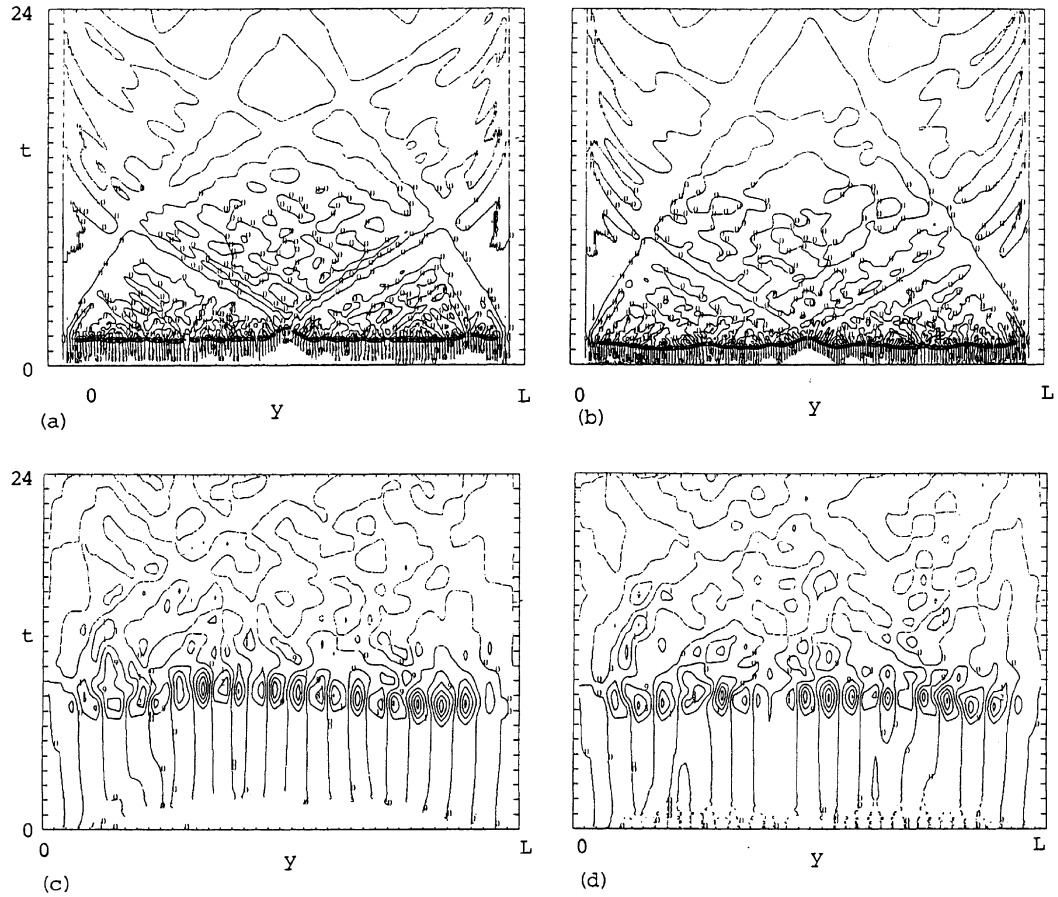

Fig. 2. The space–time (y–t) evolution of the vertical velocity at a depth of $z = 69.7$ m for hydrostatic and non-hydrostatic cases at 0.1 and 1 km resolution. The contour label is a normalized integer value between 1 and 9, which spans uniformly the minimum and maximum values of the vertical velocity $[w_{\min}, w_{\max}]$, shown for each case in cm s^{-1}; the 0-contour represents zero vertical velocity. (a) Non-hydrostatic, 0.1 km $[-20.8, 33.5]$; (b) hydrostatic, 0.1 km $[-27.9, 39.1]$; (c) non-hydrostatic, 1 km $[-5.2, 4.7]$; (d) hydrostatic, 1 km $[-4.5, 5.0]$. The tick marks on the ordinate are spaced 1 h apart.

scale ocean models, to simulate oceanic convective adjustment. We noted earlier that the hydrostatic approximation does not inhibit convection in a numerical model. For a two-layer fluid with an initial unstable stratification, a stability analysis yields the growth rates of the unstable modes (Davey and Whitehead, 1981; LD). The presence of viscosity stabilizes the smallest scales, and the horizontal scale of the most unstable mode is comparable to the vertical scale of the unstable density gradient. The most unstable modes in both hydrostatic and non-hydrostatic models are qualitatively similar, and lead to quantitatively similar convectively adjusted states in our results. Quantitatively, the hydrostatic unstable modes have a larger growth rate and are of smaller scale than their non-hydrostatic counterparts. Thus it is not the hydrostatic approximation, but rather the coarse resolution of large-scale models that limits the realistic simulation of convective adjustment.

We have simulated the convective adjustment using hydrostatic and non-hydrostatic models at moderate (1 km) and high (0.1 km) resolution. They all give qualitatively similar convectively adjusted stable states. The adjusted states can

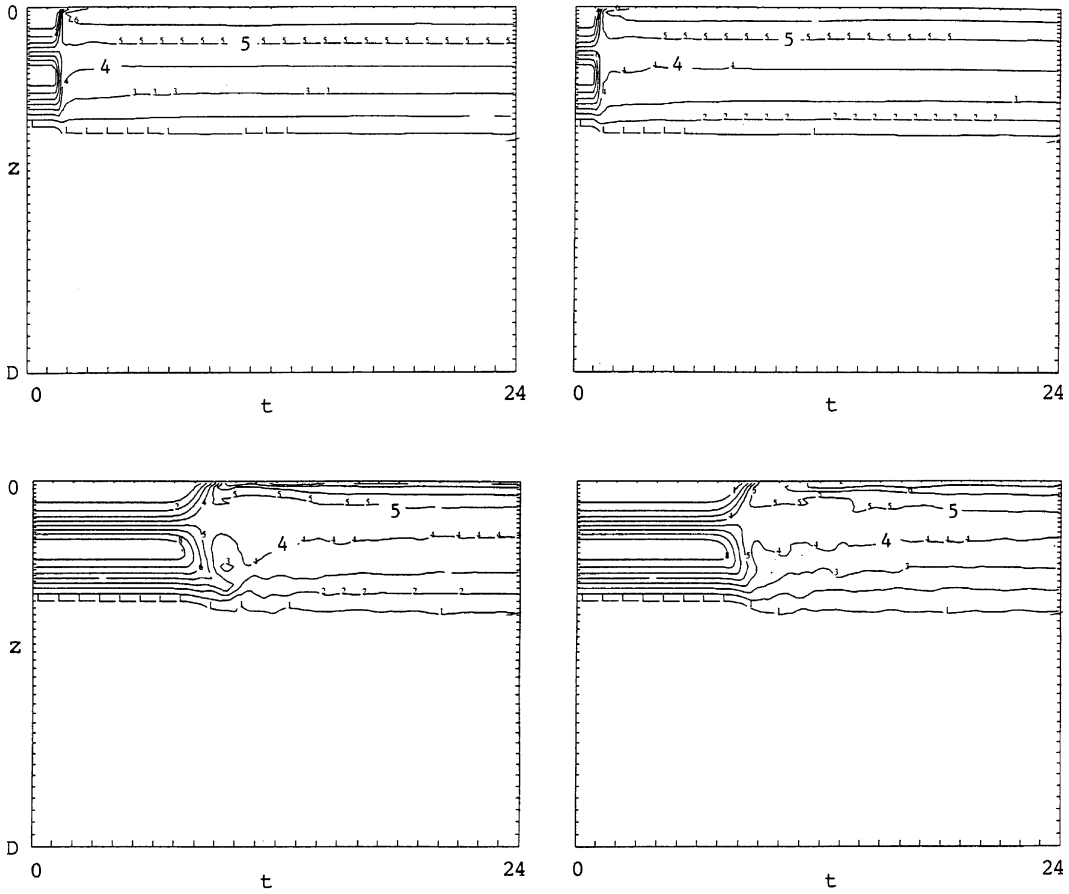

Fig. 3. The space–time (z–t) evolution of the horizontally averaged temperature field the for hydrostatic and non-hydrostatic cases at 0.1 and 1 km resolution. The contour label is a normalized integer value between 1 and 9, which spans uniformly the minimum and maximum temperature $[T_{\min}, T_{\max}] = [5.0, 9.4\,^{\circ}\mathrm{C}]$; the latter are determined by the initial conditions. (a) Non-hydrostatic, 0.1 km; (b) hydrostatic, 0.1 km; (c) non-hydrostatic, 1 km; (d) hydrostatic, 1 km. The tick marks on the abscissa are spaced 1 h apart, while those on the ordinate show the vertical grid interval increasing smoothly from 5 m at the surface to 17 m at the bottom.

have significant stratification, unlike the results obtained with instantaneous adjustment. The details of the convective plumes of course depend on whether the model is hydrostatic or not, and on resolution. The spin-up induced by the Coriolis terms inhibits convection when even lower resolution, say coarser than 10 km, is used. This effect can, however, be countered in a numerical model by the use of a vorticity filter which is strongly scale selective (Dietrich and Mehra, 1999). The main effect of the hydrostatic approximation is to create more energetic plumes, due to the removal of vertical inertia. This leads to an earlier adjusted state compared to the non-hydrostatic case. The use of coarse resolution also reduces the amplitude of the plumes, as the latter are not as well resolved. The differences between the hydrostatic and non-hydrostatic results at coarse resolution are also reduced. However, in all cases, the adjusted state is arrived at through counter-diffusive vertical advective effects, which are not captured through the use of an instantaneous adjustment. The robustness of the dynamically based convective adjustment used in LD and in the present model suggests it is a good alternative to the traditional instantaneous scheme.

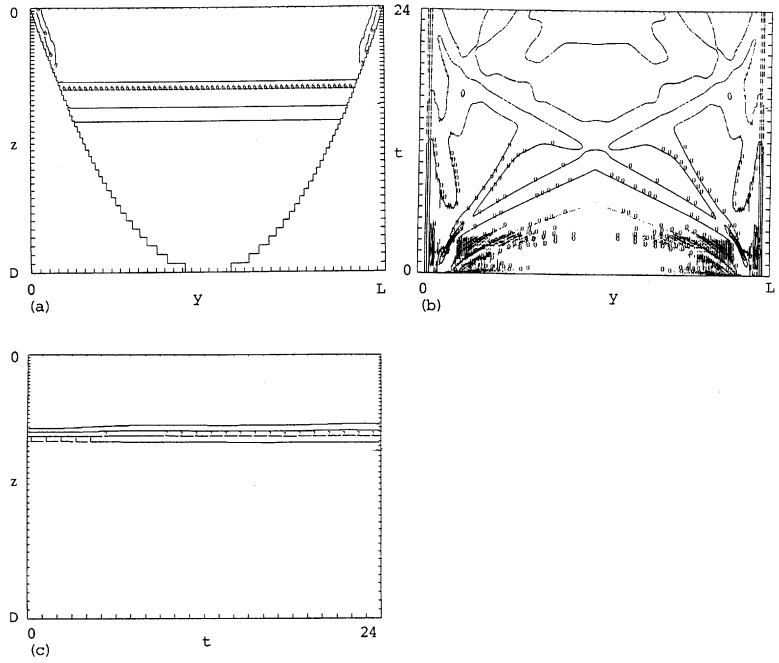

Fig. 4. The results corresponding to Figs. 1b, 2b and 3b for the hydrostatic case at 0.1 km resolution obtained with the instantaneous adjustment parameterization.

In view of the relatively low cost of including the non-hydrostatic terms and the availability of increasingly powerful computers, we recommend that ocean modelers consider the use of non-hydrostatic models, or at least models which have the non-hydrostatic option included. Our approach, and the one developed by Marshall et al. (1997), require only a modest increase of computing resources (of order 10%) to include the non-hydrostatic terms. Our recommendation may be especially useful as model resolution increases with available computing power, leading to significantly non-hydrostatic resolved modes such as those associated with convective adjustment.

5. Acknowledgements

This work is supported by grants to C. A. Lin from the Natural Sciences and Engineering Research Council (NSERC), and the Meteorological Service of Canada (MSC). The use of the computing facilities of CERCA (Centre de recherche en calcul appliqué) is gratefully acknowledged.

Appendix

We describe here the solution procedure for the non-hydrostatic incompressible flow. As mentioned earlier, we accomplish this using an iterative procedure on the local time derivative of the vertical velocity in the vertical momentum equation. All other terms in this equation are treated explicitly with no iteration, evaluated at the explicit leapfrog time level. As in the conventional hydrostatic algorithm, the vertical momentum equation is satisfied by vertical integration of the pressure gradient term, starting with a guess surface value at the rigid lid. On the 'known' right-hand side, we have the conventional buoyancy term, explicit non-hydrostatic terms and the latest iterated value of the local time derivative of the vertical velocity. The resulting pressure, when substituted into the horizontal momentum equa-

tions, generally gives a divergent barotropic mode. The standard rigid lid pressure adjustment is made to obtain a non-divergent barotropic mode. This in turn changes the advanced time level vertical velocity, and thus its local time derivative in the vertical momentum equation. The process must then be repeated iteratively to obtain convergence of the vertical momentum equation. This approach was used by Dietrich et al. (1987) to explore the adequacy of the hydrostatic approximation in the modified Arakawa C-grid SOMS model, the precursor to the DieCAST model. Dietrich and Mehra (2000) recently used the same approach to study non-hydrostatic three-dimensional convective adjustment near a shelfbreak.

Our iterative procedure to obtain the non-hydrostatic solution is numerically efficient, accurate and stable. Accurate non-divergence of the advection velocity is required to avoid false sources of the conserved variables (momentum, heat, salinity) and associated possible nonlinear numerical instability in the conservative control volume form of the conservation equations used by most models. In our iterative procedure, the advection velocity is precisely non-divergent at the end of each iteration. At this stage, the only error in the full non-hydrostatic control volume equations is due to inexact convergence of the local time derivative term in the vertical momentum equation. The local time derivative converges rapidly, and precise convergence is not needed for stability.

Even for strongly non-hydrostatic flow, the first iteration gives an accurate value for the iterated local time derivative in the vertical momentum equation, thus satisfying the full vertical momentum equation much more accurately than when using a hydrostatic approximation. The non-iterated (leapfrog) advection terms in the vertical momentum equation tend to be larger than the iterated local tendency term, thus implying even better accuracy. Thus, our procedure generally needs only one iteration per time step to get an accurate approximation of the full non-hydrostatic control volume equations. It is near optimum computationally, giving an especially big computational advantage for three-dimensional problems, because it requires only a precise solution to a two-dimensional Poisson equation to get a precisely non-divergent three-dimensional advection velocity for the next time step. Such a precise solution requires much less computation than required for the three-dimensional Poisson equation that is conventionally used to get three-dimensional incompressibility. For the two-dimensional problem addressed in this study, the Poisson equation is one-dimensional.

There is good convergence of the above procedure for the non-hydrostatic system. We have examined the various terms of the vertical momentum equation at grid points where the local vertical momentum time derivative is a maximum. The error in the vertical momentum equation is always small compared to the individual terms by several orders of magnitude, thus showing good convergence. The vertical acceleration terms are up to about 25% of the buoyancy and pressure gradient terms, indicating significantly non-hydrostatic effects.

REFERENCES

Davey, M. and Whitehead, J. A. Jr. 1981. Rotating Rayleigh–Taylor instability as a model of sinking events in the ocean. *Geophys. Astrophys. Fluid Dynam.* **17**, 237–253.

Dietrich, D. E. 1997. Application of a modified 'A' grid ocean model having reduced numerical dispersion to the Gulf of Mexico Circulation. *Dynam. Atmos. Oceans* **27**, 201–217.

Dietrich, D. A. and Mehra, A. 2000. Comparison of direct convective adjustment simulation with conventional instant convective adjustment near a shelfbreak. Center for Computational Systems Report MSSU-COE-ERC-00-08, Mississippi State University, USA.

Dietrich, D. A. and Mehra, A. 1999. Direct convective adjustment simulation using a vorticity-selective filter with application to the Black Sea. CAST Technical Report 99-1, Mississippi State University, USA.

Dietrich, D. E. and Ko, D. S. 1994. A semi-collated ocean model based on the SOMS approach. *Int. J. Num. Methods in Fluids* **19**, 1103–1113.

Dietrich, D. E., Marietta, M. G. and Roache, P. J. 1987. An ocean modeling system with turbulent boundary layers and topography. Part I: Numerical description. *Int. J. Num. Methods in Fluids* **7**, 833–855.

Fernando, H., Chen, R. and Boyer, D. 1991. Effects of rotation on convective turbulence. *J. Fluid Mech.* **228**, 513–547.

Klinger, B. A., Marshall, J. and Send, U. 1996. Representation of convective plumes by vertical adjustment. *J. Geophys. Res.* **101**(C8), 18,175–18,182.

Lin, C. A. and Dietrich, D. E. 1994. A numerical study of low Reynolds number 2-dimensional convective adjustment. *Geophys. Astrophys. Fluid Dyn.* **74**, 123–134.

Marshall, J. and Schott, F. 1999. Open ocean convection: observations, theory and models. *Rev. Geophys.* **37**, 1–64.

Marshall, J., Hill, C., Perelman, L. and Adcroft, A. 1997. Hydrostatic, quasi-hydrostatic and non-hydrostatic ocean modelling. *J. Geophys. Res.* **102**(C3), 5733–5752.

Xu, W. M. and Lin, C. A. 1993. A numerical solution of the linear Rayleigh–Benard convection equations with the B- and C-grid formulations. *Tellus* **45A**, 193–200.